STM JOURNALS

Research & Reviews: Journal of Physics
ISSN: 2278–2265 (Online), ISSN: 2347-9973 (Print)
Volume 7, Issue 3
www.stmjournals.com

Long-Period Fiber Grating Sensor to Determine Fluoride Contamination in Water

V. Jain**, *S. Kumbhaj*, *P. K. Sen
Department of Applied Physics and Optoelectronics, Shri Govindram Seksaria Institute of Technology and Science, Indore, Madhya Pradesh, India

Abstract

The spectral response of uniform long period fiber grating is analyzed theoretically considering fluoride contaminated water as its surrounding medium. The response is studied for fluoride concentration variations ranging from 1 to 20 ppm. Our analysis is based on the study of shift in resonance wavelength of the grating with change in effective refractive indices of cladding modes due to change in fluoride ion concentration in water. Results provide insight on the use of long period fiber grating for investigation of fluoride concentration in water.

Keywords: *Long-period fiber grating, refractive index, fluoride concentrations, two-layer fiber geometry*

****Author for Correspondence*** E-mail: vishaljainphysics@gmail.com

INTRODUCTION

Globally, accurate evaluation of fluoride contaminants in the drinking water has acquired great practical significance in the light of its toxic effect, which is hazardous to human health. Many epidemiological studies of possible adverse effects of the long-term ingestion of fluoride via drinking water establish that the range 1.5–10 ppm of fluoride in drinking water is cause of dental, skeleton fluorosis and excess of 10 ppm have resulted in crippling skeletal fluorosis. The problem of intake of high fluoride in drinking water has engulfed 25 nations spanning several continents such as Australia, Asia, Africa, North and South Americas. Well water containing up to 10 ppm or higher concentration have been found in many parts of India and many countries of south east Asia. In the majority of cases in India, it ranges from 1.5–6.3 ppm and in special cases, 16 to 18 ppm [1–3]. In view of this, the development of efficient, inexpensive and rapid sensing method for the detection of fluoride concentration in drinking water is gaining significant attention in the last decade. There are various chemical as well as optical techniques for the determination of fluoride impurity in water such as atomic absorption spectroscopic method [4], ion selective electrode [5], colorimetric method [6], ion chromatography [7] etc. But all the methods mentioned above require expensive and standard laboratory equipment, sample pre-treatment and mostly time consuming as well as not sensitive at lower concentration of contaminants. Thus the design and development of various fiber optic sensors have become increasingly important for numerous applications in industrial processes, biomedical analyses, and environmental monitoring. These sensors are usually employed the mechanism of evanescent field absorption [8], plasmon resonance sensing structure [9], and short and long period fiber grating [10–14].

Long period fiber gratings (LPFGs) are found to be highly sensitive to changes in its surrounding medium and, therefore, used as a refractive index sensor [15–17]. The tracing of chloride, Zn and Fe concentration in drinking and wastewater using LPFG and FBG sensors have been reported [18, 19]. In this paper, we report the spectral response of long period fiber grating to the fluoride contaminated water as the surrounding medium with the aim to design a long period fiber grating based sensor for detection of fluoride ion impurity in water.

The long period fiber gratings are periodic photo-induced devices, having refractive index modulation with period in the range of 100 µm to 1 mm and promote the coupling between fundamental core mode and co-propagating cladding modes. The high attenuation of the cladding modes results in the transmission spectrum of LPFG containing a series of attenuation bands centered at discrete wavelengths. Each attenuation band corresponds to the coupling to different cladding modes. The cladding mode is a mode supported by cladding-ambient interface and hence, the effective index of cladding mode changes with change in ambient refractive index and these result in a change in the transmission spectrum of LPFG.

Our analysis is based on the variation in coupling coefficient, resonance wavelength and transmittance of LPFG with different fluoride concentrations in water. Two-layer fiber geometry of step index fiber proposed by Vengsarkar *et al*. is used for analysis [15]. The aqueous solution of fluoride is considered as the surrounding medium. In this work, MATHCAD is used as a mathematical tool for the analysis purpose.

ANALYTICAL STUDY

Long period grating is a transmission grating whose transmission spectra exhibit several resonances resulting from coupling between fundamental core mode and different co-propagating cladding modes at wavelengths that obey the phase matching condition [17]:

$$\lambda_R = \Delta n_{eff} \Lambda = (n_{eff\,(co)} - n^m_{eff\,(cl)})\Lambda . \quad (1)$$

Where, Λ is grating period, $n_{eff\ (co),}$ and $n^m{}_{eff\ (cl)}$ are the effective refractive indices of core and the m^{th} order cladding mode of the LPFG, respectively. The $n^m{}_{eff\ (cl)}$ is ambient refractive index dependent. Hence, when the refractive index of surrounding meium changes, then a shift in the resonance wavelength can be observred. The effect of refractive index of the surrounding medium on the resonant wavelength is expressed by [19]:

$$\frac{d\lambda_R}{dn_s} = \frac{d\lambda_R}{dn^m_{cl}} \left[\frac{dn^m_{cl}}{dn_s} \right] \quad (2)$$

In Eq. (2), n_s is the refractive index of surrounding medium, which in our case is the aqueous fluoride solution. It is clear from the equation that the effective index of each cladding mode is the function of surrounding refractive index. Thus, to study the effect of aqueous fluoride solution on the spectral characteristics of LPFG, it is necessary to determine $n_{eff\ (core),}$ and $n^m{}_{eff(cl).}$ One can use two-layer model given by Vengsarkar *et al.*, and three-layer model given by Erdogen for the same [15, 20].

In our analysis, we have considered two-layer model because of its simplicity. In this model, the fiber geometry is assumed to be consisting of two concentric cylinders i.e. core and cladding, respectively (Figure 1) and effective indices are calculated using the LP mode dispersion relation as [21]:

$$u_{co}\left(\frac{J_1(u_{co})}{J_0(u_{co})}\right) = w_{co}\left(\frac{K_1(w_{co})}{K_0(w_{co})}\right). \quad (3)$$

Here, J_0 and J_1 are Bessel functions of first kind of order zero and one, respectively. K represents the modified Bessel function of second kind. u_{co} and w_{co} are the normalized transverse wave numbers related with V-parameter of fiber as:

$$u^2_{co} + w^2_{co} = V^2 \quad (4)$$

$$\text{Where, } u_{co} = a_{co}\sqrt{\left(k^2 n^2_{co} - \beta_{co}{}^2\right)} \quad (5)$$

$$w_{co} = a_{co}\sqrt{\left(\beta_{co}{}^2 - k^2 n^2_{cl}\right)} \quad (6)$$

$$V = \frac{2\pi a_{co}\left(\sqrt{n^2_{co} - n^2_{cl}}\right)}{\lambda}. \quad (7)$$

In the above equations, n_{co} and n_{cl} are refractive index of material of core and cladding of the fiber, respectively. a_{co}, β_{co}, k and λ are the core radius, core mode propagation constant, free space wave number and radiation wavelength, respectively with $k=2\pi/\lambda$.

Determination of Effective Index of Core Mode ($n_{eff(co)}$)

To determine the effective refractive index of fundamental core mode, LHS and RHS of dispersion relation Eq. (3) are plotted as functions of the transverse wave number u_{co} on the same set of axes, as shown in Figure 1.

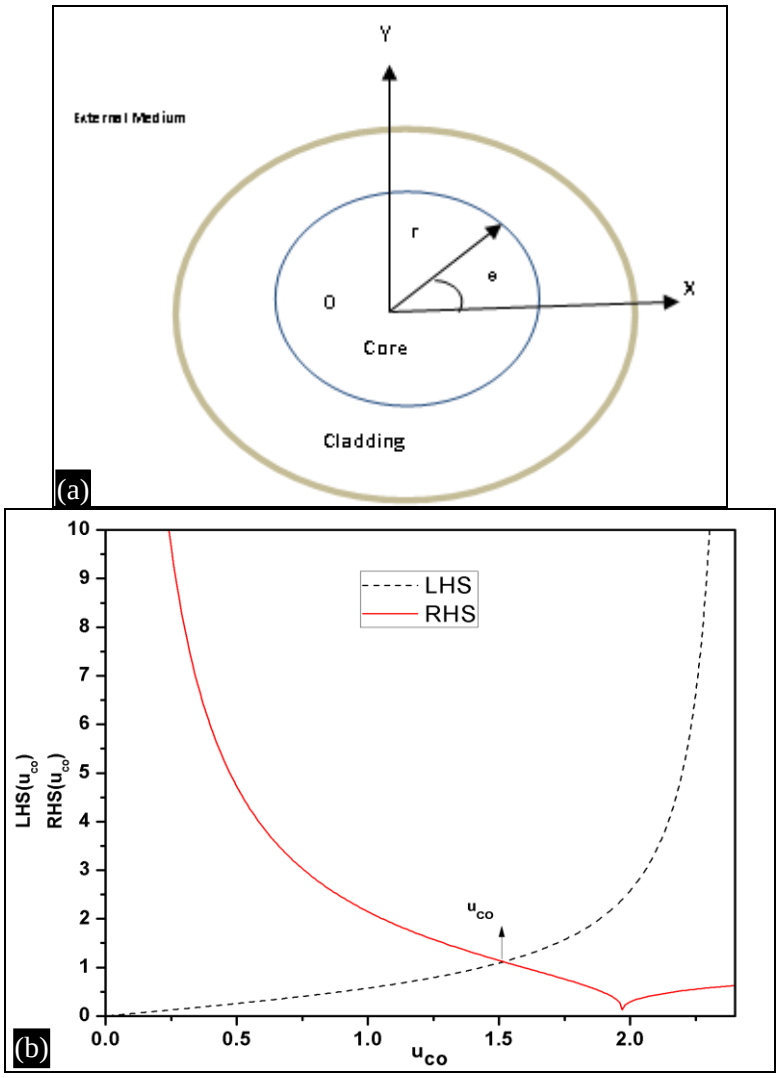

Fig. 1: a) *Cross Sectional View of an Optical Fiber, When Calculating the Core Mode;* ***b)*** *LHS and RHS of Dispersion Relation as Function of* u_{co}.

The value of 'u_{co}' at the point of intersection in Figure 1 is used in Eq. (5) to determine the core mode propagation constant (βco) and using values of βco, effective index of core is obtained by the relation:

$$n_{eff\,(co)} == \frac{\beta_{co}}{k} = \beta_{co}\frac{\lambda}{2\pi} \qquad (8)$$

Since the core mode is well coffined to the fiber core, hence, there is no variation in core effective index due to surrounding index change.

Determination of Effective Indices of Cladding Modes ($n^{m}_{eff(cl)}$)

The cladding mode effective indices are determined in the same manner as the core indices with the difference that the effect of core is assumed to be negligible at the cladding-surrounding interface. In this case, inner cylinder (core) is a homogeneous solid consisting solely of cladding material, whereas the outer cylinder (cladding) is made up of infinite and uniform medium of refractive index n_s surrounding the cladding as shown in Figure 2.

The cladding mode refractive indices are calculated by replacing the parameters u_{co}, n_{co}, a_{co} with u_{cl}, n_{cl} and $a_{cl,}$ respectively in Eqs. (3)–(7) and n_{cl} by n_s in Eqs. (6) and (7). Figure 2(a, b) shows the plot of LHS and RHS of dispersion relation for various cladding modes as a function of u_{cl}. In this case, due to large cladding radius a_{cl}, we get numerous points of intersections, each corresponding to one of several u_{cl} values belonging to specific cladding mode. The effective indices of any

m^{th} cladding mode is calculated using the expressions:

$$\beta_{cl}^{m} = \sqrt{\left(\frac{2\pi}{\lambda} n_{cl}\right)^2 - \left(\frac{u_{cl}^{m}}{a_{cl}}\right)^2}$$

$$\text{and } n_{eff(cl)}^{m} == \frac{\beta_{cl}^{m}}{k} = \beta_{cl}^{m} \frac{\lambda}{2\pi} \quad (9)$$

In the present work, we have considered the 7th cladding mode for the analysis purpose because coupling between core mode and odd cladding mode is stronger as compared to that involving the even cladding mode [20, 22]. Also, in our case, it is observed that this mode is more sensitive to the surrounding medium than its lower order modes. Variation in characteristics such as effective refractive index, resonance wavelength, coupling coefficient and transmittance of LPFG corresponding to this cladding mode is analyzed for fluoride contaminated water as surrounding medium. For this purpose, the fluoride solution is prepared by dissolving 2.2 g of sodium fluoride (NaF) in 1 l of distilled water which gives 1000 ppm of

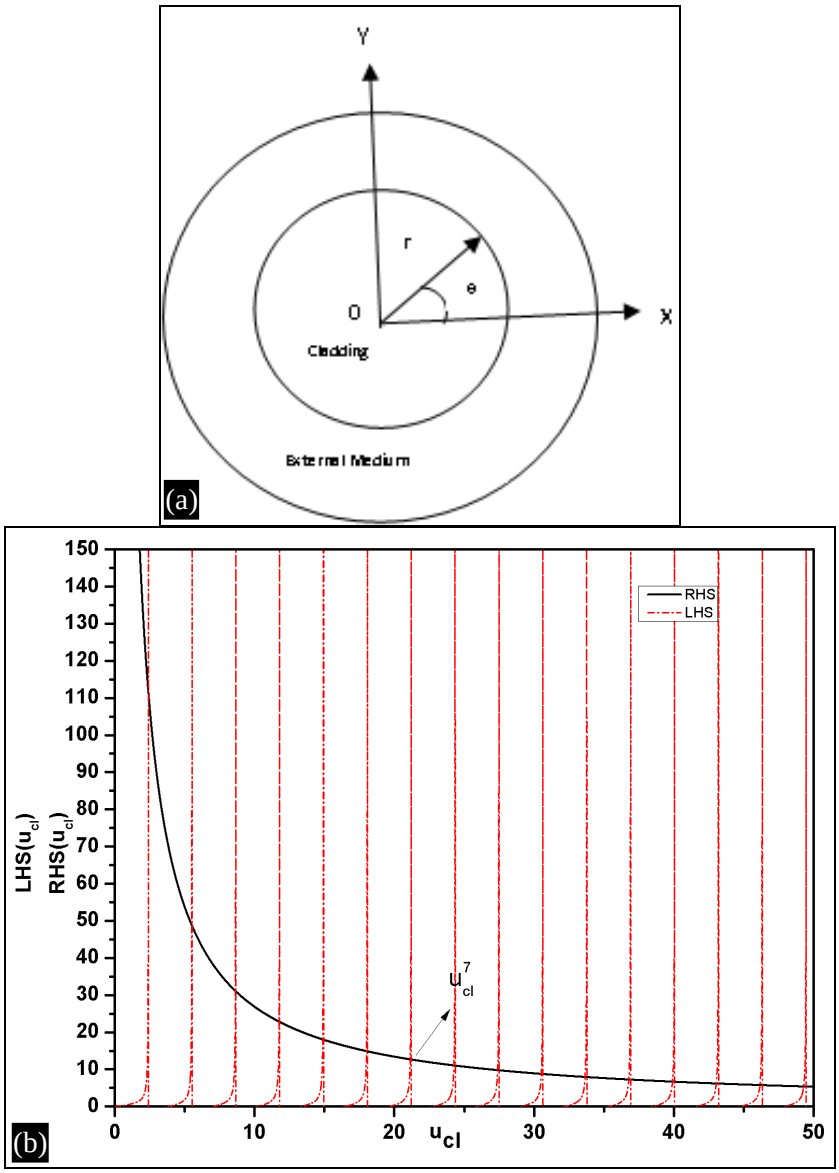

Fig. 2: (a) *Cross Sectional View of an Optical Fiber When Core Region is Ignored;* ***(b)*** *LHS and RHS of Dispersion Relation as Function of* u_{cl}.

fluoride concentration in water. The above prepared solution was then diluted to make the solutions of concentration 1, 1.5, 3.0, 5, 10, 15 and 20 ppm respectively, and corresponding refractive indices (n_s) are determined using Abbe's refractometer as given in Table 1. Using these values of n_s LHS and RHS of dispersion relation (3) are plotted as function of u_{cl}, whose modified view for 7th cladding mode is shown in Figure 3. The point of intersections are values of u^7_{cl} which are used to determine effective indices $n^7_{eff(cl)}$ with respect to various fluoride concentrations. These values of u^7_{cl} and $n^7_{eff\,(cl)}$ are indicated in Table 1.

Coupling Coefficient and Transmittance of LPFG

The transverse coupling coefficient (κ) for coupling between two co-propagating modes of azimuthally order μ and ν in uniform long period fiber grating is determined by the overlap integral of the core and cladding mode fields as [20]:

$$\kappa = \frac{\omega \varepsilon_0}{4} \int_0^{2\pi} d\phi \int_0^{\infty} r dr \Delta n \vec{E}^{t}_{\nu(r,\phi)} \vec{E}^{t}_{\mu(r,\phi)} \tag{10}$$

On mathematical simplification, Eq. (10) becomes:

$$\kappa = \varsigma \kappa^{(cl-co)}_{\nu,\mu} . \tag{11}$$

Here, ς is normalized induced core index change and $\kappa^{(cl-co)}_{\nu,\mu}$ is the coupling coefficient between the guided core and co-propagating cladding modes in the optical fiber given by [22]:

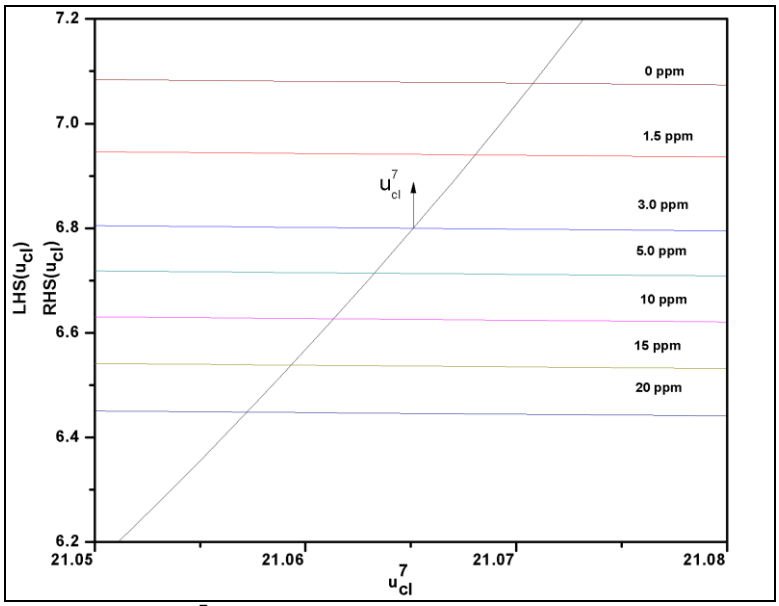

Fig. 3: *Variation in u^7_{cl} for Different Fluoride Ion Concentrations in Water.*

Table 1: *Values of u^7_{cl} Effective Indices and Resonance Wavelength at Different Fluoride Concentrations.*

Flouride Ion Concentration in Water (ppm)	n_s	u^7_{cl}	$n_{eff(cl)}$	Resonance Wavelength (λ_R) (nm)
0 ppm (Distilled water)	1.330	21.071	1.4536227	1544.5281
1.5	1.335	21.068	1.4536234	1544.2514
3.0	1.340	21.065	1.4536241	1543.9747
5.0	1.343	21.063	1.4536245	1543.8166
10	1.346	21.061	1.4536250	1543.6190
15	1.349	21.059	1.4536254	1543.4609
20	1.352	21.057	1.4536259	1543.2643

$$\kappa_{\nu,\mu}^{(cl-co)} = i\sqrt{2}\left[\frac{\gamma\rho^{1/2}J_{\mu}(Ka_{co})J_{\upsilon}(\sigma a_{co})\sqrt{\left(\frac{n_{co}}{n_{cl}}-1\right)}}{\pi a_{co}\sqrt{\left|J_{\mu-1}(Ka_{co})J_{\mu+1}(Ka_{co})\right|}\times\left|\sigma J_{\upsilon-1}(\sigma a_{co})H_{\upsilon}^{1}(\rho a_{co})-\rho J_{\upsilon}(\sigma a_{co})H_{\upsilon-1}^{1}(\rho a_{co})\right|}\right] \quad (12)$$

In the above equation, μ and ν are considered as 0 and 1 respectively. $H^{(1)}$ is the Henkel function of the first kind and the remaining wavelength dependent parameters are defined as:

$$\left.\begin{aligned}\sigma &= \sqrt{n_{co}^2k^2-\left(\beta_{cl}^{(m)}\right)^2}\\ \rho &= \sqrt{n_{cl}^2k^2-\left(\beta_{cl}^{(m)}\right)^2}\\ K &= \sqrt{n_{co}^2k^2-(\beta_{co})^2}\\ \gamma &= \sqrt{(\beta_{co})^2-n_{cl}^2k^2}\end{aligned}\right\} \quad (13)$$

Eqs. (11)–(13) reveal that coupling coefficient of LPFG depends on the refractive index of surrounding medium. Using the above relations we have calculated the values of κ for various fluoride ion concentrations in water to study the transmission characteristics of LPFG. Following relation is used to obtain the transmittance [23]:

$$T = \left[\frac{\delta^2+\kappa^2\cos^2 qL}{q^2}\right] \quad (14)$$

Here, L is the Grating length, δ and q are wavelength dependent detuning and linear dispersion parameters of LPFG and are define as:

$$\delta = \Delta n\pi\left(\frac{1}{\lambda}-\frac{1}{\lambda_R}\right) \quad q = \sqrt{\delta^2+\kappa^2} \quad (15)$$

Figure 4 is obtained by using Eq. (1) to analyze the variation of resonance wavelength of LPFG with fluoride ion concentrations such as 1, 1.5, 3.0, 5.0, 10, 15, 20 ppm in water, respectively. Figure shows that the resonance wavelength decreases with increasing concentration. This is due to the fact that the refractive index of aqueous fluoride solution increases with increasing fluoride ion concentration as indicated in Table 1.

The effect of concentration of fluoride ion on the transmittance of LPFG can be observed in Figure 5 where the transmittance of LPFG is plotted as a function of wavelength using Eq. (14). This figure reveals that there is a blue shift in transmission spectrum, whereas decrease in transmitted power decreases as we move from lower to higher concentration of fluoride in water. It is due to the combined effect of change in resonance wavelength and coupling coefficient of LPFG due to increase in effective refractive index of selected cladding mode with concentration of fluoride ion in water. The shift in the resonance wavelength is from 1544.5281 to 1543.2643 nm when the concentration of fluoride ion increases from 0 to 20 ppm. Although the spectral shift observed in this analysis are very small but can be measured using high resolution optical spectrum analyzer (better than 0.05 nm) (Table 2).

Table 2: *Physical Parameters of LPFG Corning SMF 28 Silica Glass Fiber Used for Analytical Study.*

Parameters	Values
Core refractive index (n_{co})	1.460
Cladding refractive index (n_{clad})	1.456
Core radius (a_{co})	4.5 μm
Cladding radius (a_{cl})	62.5 μm
Free space wavelength (λ)	1550 nm
Grating Length(L)	2.5 cm
Grating period (Λ)	395.25 μm
Induced index modulation (ς)	3×10^{-5}

CONCLUSION

We have analyzed the spectral response of uniform long period fiber grating (LPFG) to fluoride contaminated water as its surrounding medium. Our analysis reveals that the change in concentration of fluoride ion in water changes the position and amplitude of dip of the LPFG transmission spectrum. This analytical study suggests that an LPFG may be a potential tool to design a sensor for determination of fluoride ion concentration in drinking water.

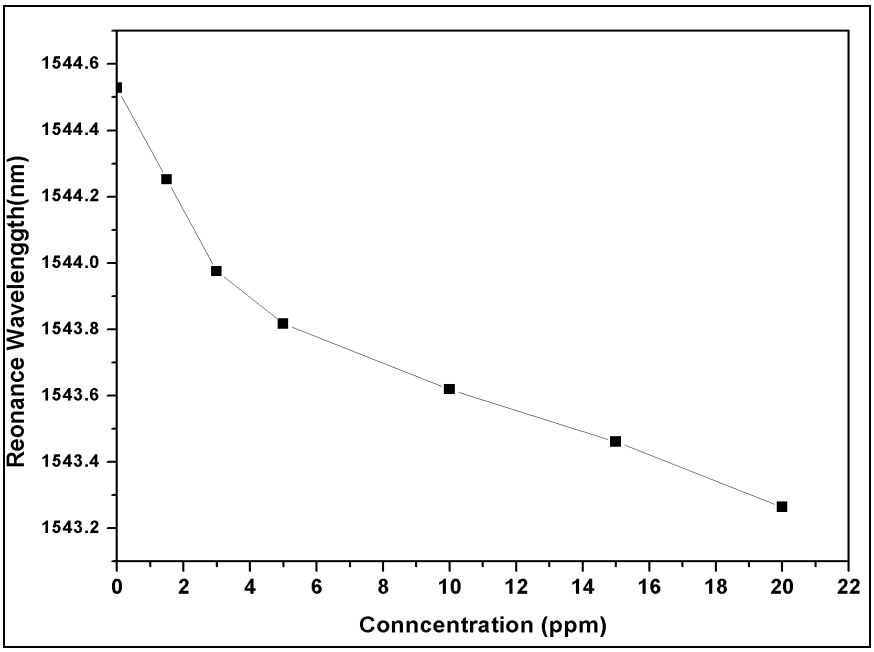

Fig. 4: *Variation in Resonance Wavelength with Fluoride Concentration in Water.*

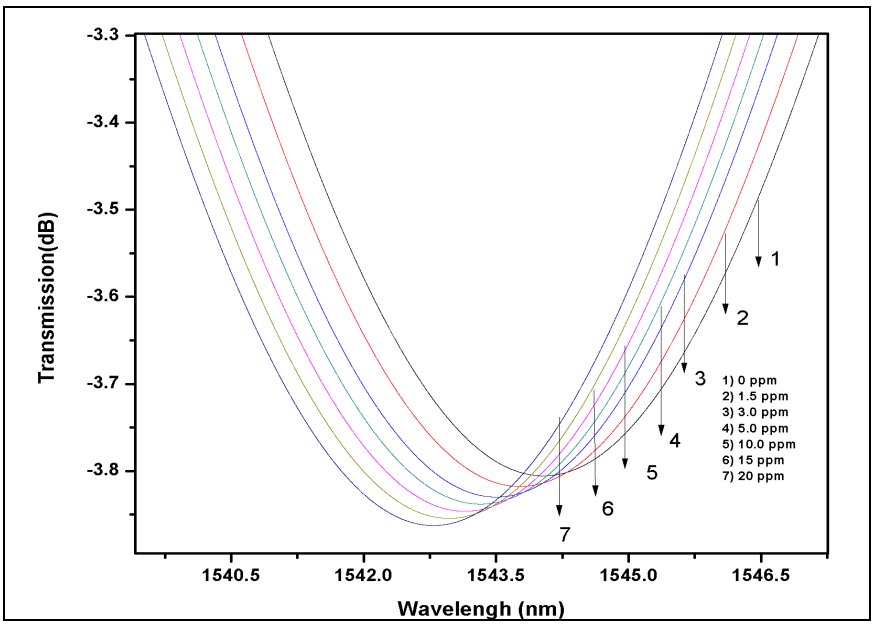

Fig. 5: *LPFG Spectrum for Different Concentrations of Fluoride Solutions.*

REFERENCES

1. Jagtap S, Yenkie MK, Labhsetwar N, *et al*. Fluoride in Drinking Water and Defluoridation of Water. *Chem Rev*. 2012; 112(4): 2454–66p.
2. Susheela AK. *A Treatise on Fluorosis*. 3rd Edn. New Delhi, India: Fluorosis Research and Rural Development Foundation; 2007.
3. Cox CR. *Operation & Control of Water Treatment Process*. Report WHO; 1969.
4. APHA, AWWA, WPCF. *Standard Methods for the Examination of Water and Waste Water*. 14th Edn. 1015 Fifteen Street, NW Washington DC: Published jointly by American Public Health Association, American Water Works Association and Water Environment Federation; 1994.
5. Alma RP, Melchor OM, Duarte G. Determination of Fluoride in Drinking Water and in Urine of Adolescents Living in Three Counties in Northern Chihuahua Mexico Using a Fluoride Ion Selective Electrode. *Microchem J*. Aug 2005; 81(1): 19–22p.

6. Chavali R, Kumar Gunda S, Naicker S, *et al.* Rapid Detection of Fluoride in Potable Water Using a Novel Fluorogenic Compound 7-O-tert-butyldiphenylsilyl-4-methylcoumarin. *Analytical Chemistry Research.* Dec 2015; 6: 26–31p.
7. Jason H, Christina L. Determination of Chloride, Fluoride, and Sulfate Ions in Various Water Samples Using Ion Chromatography. *J Anal Chem.* 2012; 3: 24–28p.
8. Kumar PS, Vallabhan CPG, Nampoori VPN, *et al.* A Fibre Optic Evanescent Wave Sensor Used for the Detection of Trace Nitrites in Water. *J Opt A Pure Appl Op*. 8 Mar 2002; 4(3): 247–50p.
9. Perrotton C, Javahiraly N, Slaman M, *et al.* Fiber Optic Surface Plasmon Resonance Sensor Based on Wavelength Modulation for Hydrogen Sensing. *Opt Express A.* 2011; 19(6): 1175–81p.
10. Wang JN, Luo CY. Long-Period Fiber Grating Sensors for the Measurement of Liquid Level and Fluid-Flow Velocity. *Sensors.* 2012; 12(4): 4578–593p.
11. Falciai R, Mignani AG, Vannini A. Long Period Gratings as Solution Concentration Sensors. *Sens Actuators B Chem.* 15 Apr 2001; 74(1–3): 74–77p.
12. Singh A, Rana SB, Singh M, *et al.* Study and Investigation of Long Period Grating as Refractive Index Sensor. *Optik: International Journal for Light and Electron Optics*. 2014; 125(7): 1860–63p.
13. Liang R, Qizhen S, Jianghai W, *et al.* Theoretical Investigation on Refractive Index Sensor Based on Bragg Grating in Micro/Nanofiber Photonics and Optoelectronics (SOPO). *Symposium on INSPEC*. 2011. Accession Number: 12034830.
14. Wang JN, Tang JL. Feasibility of Fiber Bragg Grating and Long-Period Fiber Grating Sensors Under Different Environmental Conditions. *Sensors.* 2010; 10(11): 10105–127p.
15. Vengsarkar AM, Lemaire PJ, Judkins JB, *et al.* Long Period Fiber Gratings as Band-Rejection Filters. *J Lightwave Technol*. 1996; 14(1): 58–65p.
16. Bhatia V. Applications of Long-Period Gratings to Single and Multi-Parameter Sensing. *Opt Express.* 1999; 4(11): 457–466p.
17. James SW, Tatam RP. Optical Fibre Long-Period Grating Sensors: Characteristics and Application. *Meas Sci Technol*. 2003; 14(5): 49–61p.
18. Laxmeshwara LS, Jadhava MS, Akkib Jyoti F, *et al.* Highly Sensitive Fiber Grating Chemical Sensors: An Effective Alternative to Atomic Absorption Spectroscopy. *Opt Laser Technol.* 2017; 91: 27–31p.
19. Laxmeshwara LS, Jadhava MS, Akkib Jyoti F, *et al.* Quantification of Chloride and Iron in Sugar Factory Effluent Using Long Period Fiber Grating Chemical Sensor. *Sens Actuators B Chem.* Apr 2018; 258: 850–856p.
20. Erdogan T. Cladding-Mode Resonances in Short- and Long-Period Fiber Grating Filters. *J Opt Soc Am A.* 1997; 14(8): 1760–73p.
21. Ghatak A, Thyagarajan K. *Optical Electronics*. Cambridge: Cambridge University Press; 1989.
22. Marcuse D. *Theory of Dielecric Optical Waveguides.* New York: Academic Press; 1974.
23. Kutz JN, Eggleton BJ, Stark JB, *et al.* Nonlinear Pulse Propagation in Long-Period Fiber Gratings: Theory and Experiment. *J Sel Topics Quantum Electron*. 1997; 3(5): 1232p.

Cite this Article

Jain V, Kumbhaj S, Sen PK. Long-Period Fiber Grating Sensor to Determine Fluoride Contamination in Water. *Research & Reviews: Journal of Physics*. 2018; 7(3): 36–43p.